

Opportunistic Adaptive Haptic Sampling on Forward Channel in Telehaptic Communication

Vineet Gokhale * Jayakrishnan Nair** Subhasis Chaudhuri***
Indian Institute of Technology Bombay

Abstract— We propose a network-based opportunistic improvisation to adaptive sampling for the forward channel telehaptic data stream on a time-varying network. The algorithm explores real-time tuning of the perceptual deadband parameter to minimize network underutilization, and consequently improves the quality of telehaptic communication. We describe in detail the rationale behind the design choices of the proposed sampling scheme. We perform both real-time telehaptic experiments and simulations to test the proof of concept. The reconstructed haptic signals reveal a substantial improvement in average SNR of 3.57 dB, suggesting that the proposed method outperforms the conventional adaptive sampling technique to a large extent. In addition to satisfying the telehaptic Quality of Service (QoS) requirements, we also demonstrate that our method does not overwhelm the network or penalize the concurrent traffic streams.

Keywords - Telehaptics, opportunistic, adaptive sampling, forward channel, throughput, SNR

I. INTRODUCTION

Telehaptic applications involving exploration/manipulation of remote objects using haptic, auditory, and visual feedbacks place very strict timing constraints on the multimedia data delivery. Haptic information being the most delay-sensitive amongst the aforementioned media types, necessitates a very high speed data transfer across the communication medium. Studies have shown that the Quality of Service (QoS) - allowable limits on the end-to-end delay, jitter and packet loss - for the haptic media are 30 ms, 10 ms and 10%, respectively [1], [2], [3]. A violation of the haptic QoS constraints potentially causes instability of the haptic control loop, and a perceivable impairment of the telehaptic activity.

Guaranteeing the stringent QoS requirements of the telehaptic applications is challenging over a shared network, like the Internet, since the telehaptic application has to compete for network resources with other concurrent traffic flows. Moreover, the network cross traffic is itself time varying, making the problem even more challenging.

Several previous works on telehaptic communication use haptic data packetization at the default sampling rate of 1 kHz, resulting in 1000 packets/sec and a data rate in the neighborhood of 700 kbps or more (the precise rate depends on the networking standards and the application layer overheads); see, for example, [4], [5], [6]. Transmission at such a high data rate works well when the network is relatively

uncongested. However, during periods of network congestion, this can lead to large packet delays and/or frequent packet drops, making the telehaptic application susceptible to QoS violations. Transmission at the peak data rate is also problematic in resource constrained networks, such as wireless adhoc networks deployed for disaster management.

In order to overcome the risk of QoS violations, researchers have proposed a variety of haptic data compression techniques; see, for example, [7], [8], [9], [10], [11], [12]. In this paper, we consider the technique in [8] called adaptive sampling - a human perception based technique that examines the percentage change in magnitude between the current and a reference haptic sample. If this percentage change exceeds a certain threshold p , known as adaptive sampling threshold, then the current sample is marked as significant in terms of signal reconstruction at the receiver. For example, $p = 10\%$ means that the current haptic sample is significant only if its magnitude is greater (lesser) than 1.1 (0.9) times the reference magnitude. Hence, a substantial haptic compression is achieved by not transmitting the insignificant samples. Adaptive sampling is applied on the velocity and force updates on the forward (operator to teleoperator) and backward channels (teleoperator to operator), respectively. For example, the work in [8] shows an overall reduction in the haptic data rate of 75% on the forward channel and 90% on the backward channel with the adaptive sampling thresholds $p = 25\%$ and 10%, respectively. For convenience, we refer to adaptive sampling schemes with a fixed p for a telehaptic session as *static adaptive sampling*.

However, in critical applications like telesurgery and tele-maintenance, the teleoperator is a robotic device that receives position-velocity updates to reproduce the activity of the operator as precisely as possible. In presence of high-precision actuators, the teleoperator can execute even the slightest of position-velocity changes. Thus, in such cases, the use of adaptive sampling, a technique based on human perceptual limitations, on the forward channel from the operator to a robotic teleoperator, is suboptimal, as the full precision of the teleoperator is never exploited.¹ This suboptimality is particularly significant when the network is uncongested, since transmitting haptic data at the peak data rate would lead to a better reproduction of the operator's actions by the teleoperator.

To summarize, the literature proposes two extreme tech-

*email: vineet@ee.iitb.ac.in

**email: jayakrishnan.nair@ee.iitb.ac.in

***email: sc@ee.iitb.ac.in

Funding supports from Indian Digital Heritage project, Bharti Centre for Communication and NPPE programs are gratefully acknowledged.

¹However, the deadband approach works well in the backward channel due to the human operator on the receiving end.

niques for telehaptic communication over a network. On one hand, transmitting haptic data at the peak rate works well when the network is uncongested, but is problematic when the network is congested. On the other hand, adaptive sampling works well when the network is congested, but is suboptimal when the network is uncongested, especially in applications where the teleoperator is a robotic device. The key issue with both the aforementioned approaches is that they are insensitive to the state of congestion of the network. This motivates us to consider opportunistic schemes for telehaptic communication that adapt their transmission rate depending on the level of congestion in the network.

In this work, we propose a network-based opportunistic method for adaptive sampling on the velocity updates at the operator. In addition to satisfying the haptic QoS specifications, the goal of the opportunistic scheme is to maximize the transmitted haptic packet rate, subject to network resource constraints. The assumption here is that at any point in time, the network supports the minimum haptic data rate corresponding to static adaptive sampling. By monitoring the end-to-end delays on the forward channel, we estimate the congestion level in the network, and the *opportunistic adaptive sampling* algorithm appropriately adapts the adaptive sampling threshold p . The method is opportunistic as it constantly looks for an opportunity to pump more haptic packets without violating the QoS constraints. To validate our approach, we record real-world haptic signals using a real-time telepottery experiment with several human subjects. We conduct simulations on the recorded signals, using a discrete event network simulator NS3 [13]. Our experiments demonstrate a substantial improvement in the packet rate as well as the reconstructed velocity signal at the teleoperator, compared to static adaptive sampling. Additionally, we analyze the interplay between the telehaptic traffic and other network sources, and conclude that the opportunistic algorithm is friendly to exogenous cross traffic flows, in terms of resource sharing.

II. TYPICAL TELEHAPTIC ENVIRONMENT

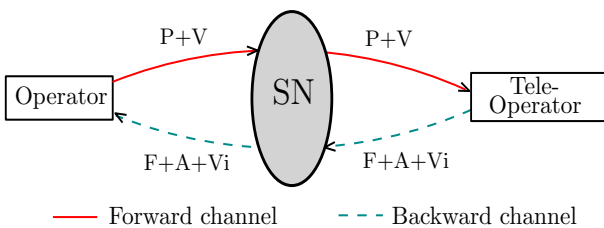


Fig. 1: Representation of a telehaptic setup on a shared network. Notations used: SN - shared network, P - position, V - velocity, F - force, A - audio, Vi - video.

In this section, we describe a typical telehaptic environment using a point-to-point application model shown in Figure 1. The operator transmits the position-velocity information corresponding to the hand movements to the teleoperator on the forward channel. On reception of the position-velocity commands, the teleoperator follows the trajectory created by the operator. The interaction forces

generated between the teleoperator and the remote objects are transmitted to the operator on the backward channel. Additionally, the teleoperator transmits auditory and visual information of the remote scene. In a realistic scenario, the telehaptic traffic can encounter asymmetric network behavior, which means that the forward and backward channels can have non-identical end-to-end delays, jitter and packet losses. The asymmetric behavior is primarily due to the different network traffic conditions, as well as different routing and buffering schemes at the intermediate routers on the two channels.

III. THE PROPOSED SAMPLING FRAMEWORK

In this section, we describe in detail the constituent modules of the proposed opportunistic adaptive sampling method; see Figure 2.

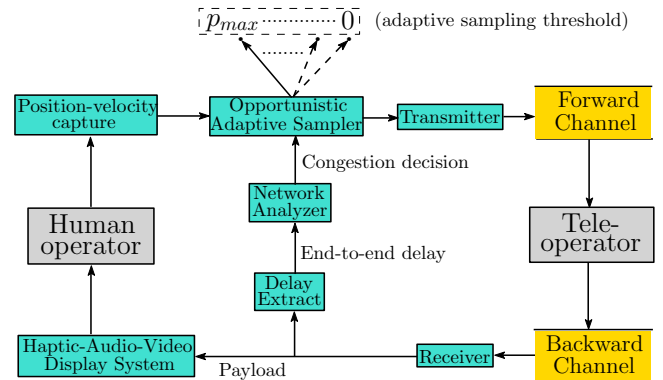


Fig. 2: Block diagram representation of the communication module showing the proposed sampling framework for the forward channel.

A. Network Analyzer

It is essential for the operator to be aware of the congestion on the forward channel so as to be able to carry out adaptation of the telehaptic data rate. The end-to-end delays on the forward and backward channels are different due to the asymmetric behavior of the channels. Therefore, the end-to-end delays on the backward channel do not convey the state of congestion on the forward channel. We exploit the bidirectional nature of the telehaptic communication for notifying the operator of the forward channel delays. The forward channel monitoring is carried out by the *network analyzer*. We use the end-to-end delay on the forward channel as an indicator of congestion. The forward channel end-to-end delays are measured at the teleoperator based on packet timestamps, and are piggybacked as part of the headers in the telehaptic packets transmitted on the backward channel. The trends followed by the end-to-end delays precisely suggest network congestion or underutilization. For network monitoring, we use an exponentially weighted moving average filter on the end-to-end delays defined by

$$d_{avg}(m) = \beta * d_{avg}(m-1) + (1-\beta) * d(m), \quad (1)$$

where $0 < \beta < 1$. Here, $d(m)$ and $d_{avg}(m)$ denote the m 'th end-to-end delay and m 'th weighted average delay

measurement, respectively. If $d_{avg}(\cdot)$ shows N continuous increasing measurements, then the network is detected to be congested. If the end-to-end delays do not manifest a continuous increase or decrease, then the network is in an uncongested state. Upon detection of presence or absence of congestion, the network analyzer updates a flag C called the *congestion decision* to 1 or 0, respectively. The filter described by Equation 1 is reset after each update. Further details on the end-to-end delay trend detection and piggy-backing mechanism are not included in the paper due to space constraints. The use of data packets in the backward channel as carriers of the forward channel end-to-end delay provides a very fast estimate of the network congestion state without incurring much additional packet overhead, thus enabling quick adaptations to the fluctuating network conditions. In our simulations (see Section V), we set $\beta = 0.6$ and $N = 10$.

B. Opportunistic Adaptive Sampler

The objective of the *opportunistic adaptive sampler* is to transmit as many haptic packets as the network supports at a given instant. It achieves this by dynamically tuning the adaptive sampling threshold, based on the congestion decision C . Note that increasing the adaptive sampling threshold results in a wider deadband, which in turn results in a lower haptic data rate.

The adaptive sampling threshold p (in %) is varied over the range $[0, p_{max}]$ in steps of γ . Here, p_{max} and γ are algorithm parameters, with p_{max} being an integral multiple of γ . The opportunistic adaptive sampler updates the current adaptive sampling threshold, denoted by p_{curr} , each time the congestion decision C is updated, as follows.²

If $C = 1$ the opportunistic adaptive sampler sets $p_{curr} = p_{max}$. In other words, when congestion is detected, the algorithm aggressively cuts its data rate to the lowest level permissible. This is in line with the classical additive-increase/multiplicative-decrease (AIMD) approach [14] in network congestion control literature. Indeed, the signal $C = 1$ suggests that the buffers at the intermediate routers on the forward channel are either fast filling or overflowing. Thus, a rapid transmission rate reduction enables the network buffers to clear, and minimizes the chance of QoS violations.

If $C = 0$, then the opportunistic adaptive sampler reduces the adaptive sampling threshold p_{curr} by γ (in %), so long as $p_{curr} > 0$. The algorithm takes $C = 0$ as a signal that the network is uncongested, and thus attempts to increase the haptic data rate. The increase in the haptic data rate is performed in a controlled, multistep manner, also in line with the AIMD approach.

To summarize, the update of the current adaptive sampling threshold p_{curr} is performed as follows.

$$p_{curr} \leftarrow p_{max} * C + (1 - C) * [\mathbf{1}_{(p_{curr} > 0)} * (p_{curr} - \gamma)].$$

Here, $\mathbf{1}_{(Z)}$ equals 1 if Z is true and 0 otherwise.

²Any instance of detection of presence/absence of congestion is considered to be an update. Note that the value of C need not change at an update.

The opportunistic sampler operates at an initial $p_{curr} = p_{max}$ as the network condition is unknown at the beginning of the telehaptic session, and it is safer to the start transmission at the minimal haptic data rate.

Time-Out Strategy: The forward channel end-to-end delays are measured at the teleoperator only upon haptic packet reception. The freshly calculated delays are then piggy-backed on the force-audio-video packets transmitted on the backward channel. This means that the operator can learn the forward channel condition only when it transmits new packets. During intervals when the operator carries out very slow hand movements, adaptive sampling at threshold p_{curr} might discard several successive haptic samples, giving rise to a long period without any transmissions from the operator. This in turn results in a long period where the operator is starved of feedback on delays on the forward channel, thus temporarily pausing the adaptive sampling threshold adjustment.

To circumvent this condition, the operator starts a timer after the latest haptic packet transmission. If the time elapsed after the latest transmission exceeds the time-out interval, denoted by T_o , then the operator reads a haptic sample directly from the device drivers and transmits it, irrespective of its significance. After the transmission, the timer is restarted. This strategy ensures that the operator is not starved of the end-to-end delay feedbacks, and thereby avoids network underutilization.

IV. EXPERIMENTAL SETUP

In this section, we describe the setup of our experiments to assess the performance of the proposed telehaptic transmission scheme.

A. Haptic Data Generation

We leverage a real-time telepottery model [5] to generate real-world telehaptic signals. In a real-time telepottery system, the human operator manipulates a remotely rendered volume conserving pottery object [15] using audio, video and haptic information from the remote scene. Eight human subjects, six males and two females, aged between twenty three and fifty two years participated in the telepottery experiment. Out of them, three were regular users of the haptic devices. Nevertheless, ample time was provided to the subjects prior to data collection to get accustomed to the telehaptic environment. During the data collection phase, we record the velocity traces generated by each of the subjects over the telepottery interaction.

B. NS3 Simulation Testbed

The velocity traces captured during the telepottery interaction are utilized in NS3 simulations for evaluating the performance of the opportunistic adaptive sampling scheme. The shared network topology used in the simulations is shown in Figure 3.

The unidirectional links have a capacity of 1500 kbps. The one-way propagation delay between the operator and

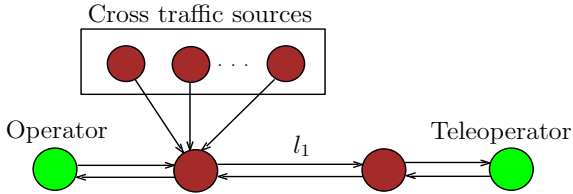


Fig. 3: Network topology designed for the simulations. l_1 - bottleneck link on the forward channel.

the teleoperator is configured to 12 ms, thus resulting in a round-trip propagation delay of 24 ms. We choose $p_{max} = 30\%$, $\gamma = 2\%$, and $T_o = 20$ ms for our experiments. We compare our opportunistic scheme with static adaptive sampling operating at a fixed threshold of $p = 30\%$. Due to the chosen network configuration, l_1 acts as the bottleneck link on the forward channel. At the teleoperator, a zero-hold strategy is used for haptic signal reconstruction.

V. EXPERIMENTAL RESULTS

In this section, we evaluate the performance of the opportunistic sampler in terms of the haptic QoS conformance, and enhancement of the reconstructed haptic signal at the teleoperator. Additionally, we assess the friendliness of the algorithm to the concurrent traffic streams in the network.

A. Telehaptic-CBR Cross Traffic Interplay

In this section, we carry out detailed study of the interplay between telehaptic and constant bitrate (CBR) cross traffic.

1) *SNR-Throughput Measurements*: Each of the recorded velocity signals are initially transmitted on a 100 Mbps network, and the corresponding reconstructed velocity signals are considered as benchmark, for each specific human subject. For convenience, we denote the CBR cross traffic intensity on the forward channel as R_{cbr} .

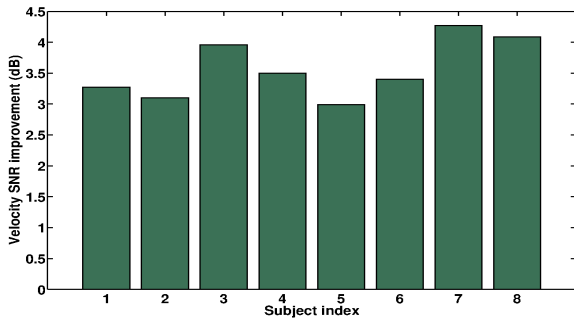


Fig. 4: SNR improvement of opportunistic over static adaptive sampling measured for the velocity updates.

First, we discuss the SNR improvement achieved by the proposed opportunistic sampler over the static adaptive sampler across the different real-world velocity traces. For these simulations, we set $R_{cbr} = 980$ kbps. Our results are presented in Figure 4. Note that the opportunistic sampler achieves an average SNR improvement of 3.57 dB over the static adaptive sampling strategy. This is because the static method underutilizes the network, and loses out on the possibility of transmitting a higher resolution haptic

signal. Our proposed method opportunistically senses the available bandwidth in the network and transmits a higher haptic data rate, while still complying with the telehaptic QoS constraints.

Next, we study the gain in telehaptic throughput and the SNR improvement of the proposed method over the static adaptive sampler over a range of CBR cross traffic intensity. From now on, for brevity, we only present the results corresponding to the velocity trace generated by Subject 5. However, the nature of the findings remains consistent across subjects.

The haptic data rate due to the static adaptive sampling for Subject 5 turns out to be 221 kbps. Figure 5 demonstrates the correlation between the telehaptic throughput and SNR improvement of the opportunistic sampler over the static adaptive sampling scheme. It can be observed that for $R_{cbr} \leq 804$ kbps, the opportunistic scheme achieves the peak haptic data rate of 696 kbps, thereby resulting in a near error-less signal reconstruction.³ The SNR improvement is very large in this range (not captured in the figure) as the error between the benchmark signal and the reconstructed signal due to the opportunistic sampling is negligible.

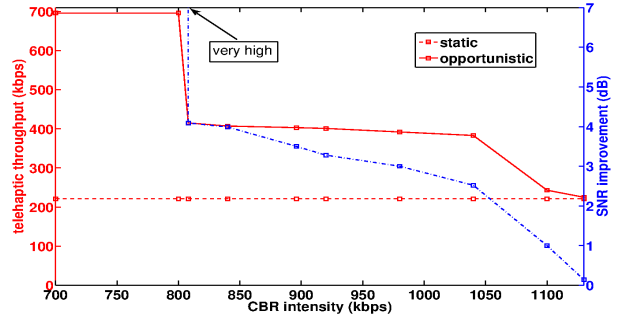


Fig. 5: Telehaptic throughput adaptation along with the corresponding SNR improvement over static adaptive sampling for a real-world velocity signal.

As R_{cbr} is increased from 804 to 1130 kbps, the opportunistic scheme gradually reduces its transmission rate, thus ensuring that the concurrent flows are not throttled. Consequently, the SNR improvement over the static adaptive sampler also reduces gradually with increasing R_{cbr} . We note that the CBR flow attains full throughput and sustains no losses over this range of R_{cbr} , though this is not apparent from the figure. For $R_{cbr} > 1130$ kbps, the opportunistic scheme is unable to transmit at a rate higher than the static adaptive sampler, and is consequently unable to produce an SNR improvement.

To demonstrate that our opportunistic scheme meets the telehaptic QoS requirements, Table I gives a comparison of the experimental observations and the corresponding QoS limits of the end-to-end delays and jitter, with $R_{cbr} = 1100$ kbps. Note that the haptic flow does not lose any packets. Thus, we conclude that even under very high cross traffic

³It turns out that in our setting, the peak haptic data rate on the forward channel equals 696 kbps. Thus, 804 kbps is the largest possible network cross traffic data rate such that the haptic source can transmit at its peak rate, given that the bottleneck link has a capacity of 1500 kbps.

		End-to-end delay (ms)	Jitter (ms)
QoS		30	10
Expt.	Max	23.995	0.636
	Avg	16.645	0.165

TABLE I: QoS performance of the proposed opportunistic scheme when $R_{cbr} = 1100$ kbps.

intensity, the opportunistic scheme adheres well to the QoS specifications.

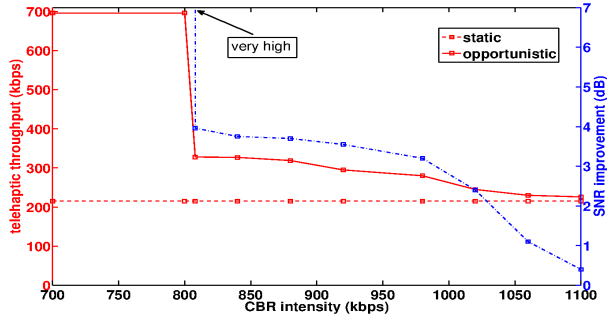


Fig. 6: Telehaptic throughput adaptation along with the corresponding SNR improvement over static adaptive sampling for a synthetic velocity signal.

Finally, we evaluate the performance of the proposed sampler for a synthetic velocity trace generated using a standard statistical model, in order to provide a task or subject independent analysis of its performance. For this purpose, we generate a white Gaussian signal, smoothed using a simple moving average filter with a cutoff frequency of 100 Hz. We feed this signal in place of the velocity trace generated by the operator, and test the performance of the proposed sampler over a wide range of mean and standard deviation of the source Gaussian signal. For brevity, we report the observations for mean and standard deviation of 0.3 cm/s and 0.3 cm/s, respectively. The chosen values are realistic, since rapid hand movements are unlikely to occur in a practical telehaptic application. Figure 6 presents the telehaptic throughput and SNR improvement of the proposed sampler as a function of R_{cbr} . We note that the results are quite similar to those from the subject trace as shown in Figure 5. This demonstrates that the performance enhancement of the opportunistic adaptive sampler is robust with respect to the haptic source.

2) *Temporal Behavior*: We now describe the temporal behavior of the proposed opportunistic adaptive sampler. Throughout this section, we use the velocity trace corresponding to Subject 5.

First, we depict the temporal variation of the end-to-end delays and the adaptive sampling threshold p_{curr} . For this experiment, we set $R_{cbr} = 1100$ kbps. The sample-wise end-to-end delay encountered by the velocity updates, along with the corresponding p_{curr} is presented in Figure 7. It can be observed that when the forward channel is uncongested, the delays exhibits a steady behavior, and the opportunistic algorithm reduces the adaptive sampling threshold p_{curr} based on the threshold update scheme presented in Section

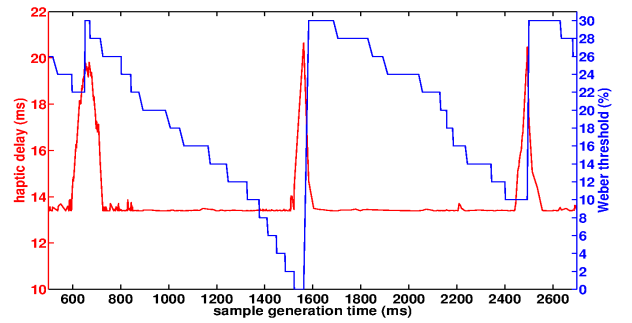


Fig. 7: End-to-end delay encountered by the haptic samples, along with the corresponding adaptive sampling thresholds.

III-B. It is clear from the graph that when the network is congested, the algorithm performs a quick congestion control through the aggressive fall back approach without significantly building up the delay. The switch to p_{max} is deferred after the start of a delay build-up (for example, from 600 ms to 650 ms) primarily due to the propagation delays of the forward and the backward channels. The periods where $p_{curr} < p_{max}$ are when the opportunistic scheme transmits at a higher rate than the static adaptive sampler, resulting in a better velocity signal reconstruction compared with the static adaptive sampler.

Next, we present the temporal variation in the haptic packet rate, when the cross-traffic is time-varying. We simulate two CBR cross traffic sources on the forward channel: C_1 with a data rate of 900 kbps, and C_2 with a data rate of 200 kbps. We use different combinations of the two CBR sources to design a cross traffic scheme as shown in Equation (2).

$$R_{cbr} = \begin{cases} 0, & \text{for } 0 < t \leq 3s \\ 900 \text{ kbps } (C_1), & \text{for } 3 < t \leq 5s \\ 1100 \text{ kbps } (C_1 \text{ and } C_2), & \text{for } 5 < t \leq 7s \\ 200 \text{ kbps } (C_2), & \text{for } t > 7s \end{cases} \quad (2)$$

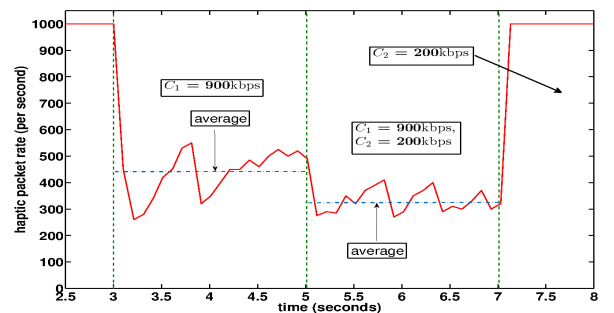


Fig. 8: Temporal behavior of the haptic packet rates due to the opportunistic algorithm under intermittent CBR cross traffic conditions.

Our results are shown in Figure 8. Until 3 seconds, the telehaptic source transmits at 1000 packets/sec as there are no concurrent flows on the forward channel. After 3 seconds, the available capacity on the forward channel is insufficient to sustain the peak haptic data rate. Accordingly,

the opportunistic scheme dynamically lowers its packet rate. The reduction in the haptic packet rate due to CBR source C_1 alone is clearly observable between 3 and 5 seconds. At 5 seconds, the additional traffic due to the CBR source C_2 results in a further reduction in the haptic packet rate. C_1 aborts transmission at 7 seconds, after which point the telehaptic source resumes transmission at 1000 packets/sec.

B. Telehaptic-TCP Cross Traffic Interplay

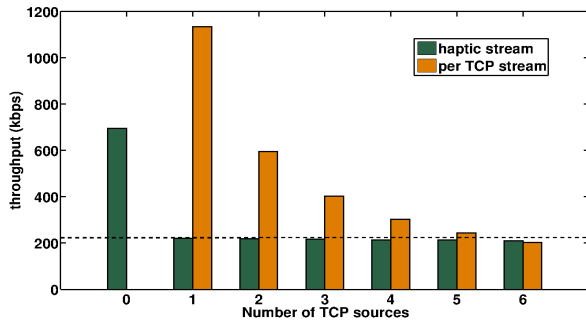


Fig. 9: Demonstration of TCP-friendliness of the opportunistic algorithm.

In this section, we study the interaction of our proposed scheme with Transmission Control Protocol (TCP) cross-traffic. As before, we use the velocity trace generated by Subject 5. Figure 9 presents the haptic and TCP throughput per stream, for a varying number of TCP NewReno streams, each with an infinite backlog of data. In absence of TCP flows, the telehaptic source gains its peak throughput of 696 kbps. It is clear from the graph that in presence of TCP sources, the telehaptic source attains a maximum throughput of 221 kbps. The presence of multiple TCP sources increases packet drops in the network. Therefore the telehaptic throughput gradually reduces even though the telehaptic source rate remains at 221 kbps. Thus, in the presence of TCP cross-traffic, our opportunistic scheme backs off to its minimum rate. This is because our opportunistic sampler has a much faster response to network changes as compared to TCP. Due to this, the telehaptic source responds to congestion much earlier than the TCP sources, resulting in haptic data rate back-off. On the other hand, the TCP sources, being more sluggish in their congestion response, benefit from this early back-off by the telehaptic stream.

Thus we conclude that the proposed opportunistic adaptive sampling scheme is highly TCP-friendly, albeit at the cost of QoS violations. A finer analysis of the interplay between telehaptic congestion control and TCP is beyond the scope of the present paper, and represents an interesting avenue for future work.

VI. CONCLUSIONS AND FUTURE WORK

In this work, we explored a possible solution for enhancing the telehaptic communication based on an opportunistic network utilization approach on the forward channel. We demonstrated that the proposed algorithm enhances the telehaptic throughput by a fairly considerable extent, without overwhelming the underlying shared network. The results

presented show haptic QoS adherence under adverse cross traffic scenarios. The SNR measurements reveal that the opportunistic adaptive sampler outperforms the static adaptive sampler in terms of the quality of signal reconstruction at the teleoperator. We also demonstrated the cross-traffic friendliness behavior of the opportunistic scheme. The aforementioned characteristics make the opportunistic adaptive sampler a potential sampling scheme for delay-critical telehaptic applications on a time-varying network.

In this paper, the opportunistic adaptive sampling scheme is assumed to be independent of the statistics of the haptic data generation process. The possibility of tuning the rate adaptation to the data statistics would be an interesting problem. Also, the implication of the SNR improvement on the precision of the telehaptic task is yet to be investigated. We also intend to extend the idea of opportunistic sampling to other type of adaptive sampling schemes, for example, level crossings [10].

REFERENCES

- [1] A. Marshall, K. M. Yap, and W. Yu, "Providing qos for networked peers in distributed haptic virtual environments," *Advances in Multimedia*, 2008.
- [2] S. Matsumotoy, I. Fukuday, H. Morinoy, K. Hikichiy, K. Sezakiz, and Y. Yasuda, "The influences of network issues on haptic collaboration in shared virtual environments," in *Proceedings of the 5th Phantom Users' Group Workshop*, 2000, pp. 22–24.
- [3] Y. Ishibashi and H. Kaneoka, "Fairness among game players in networked haptic environments influence of network latency," in *IEEE International Conference on Multimedia and Expo (ICME)*, 2005., 2005.
- [4] M. Eid, J. Cha, and A. El Saddik, "Admux: An adaptive multiplexer for haptic-audio-visual data communication," *IEEE Transactions on Instrumentation and Measurement*, vol. 60, no. 1, pp. 21–31, 2011.
- [5] V. Gokhale, S. Chaudhuri, and O. Dabeer, "HoIP: A point-to-point haptic data communication protocol and its evaluation," in *Twenty First National Conference on Communications (NCC)*. IEEE, 2015, pp. 1–6.
- [6] V. Gokhale, O. Dabeer, and S. Chaudhuri, "HoIP: Haptics over internet protocol," in *IEEE International Symposium on Haptic Audio Visual Environments and Games (HAVE)*, 2013, pp. 45–50.
- [7] N. Sakr, N. D. Georganas, and J. Zhao, "Human perception-based data reduction for haptic communication in six-dof telepresence systems," *IEEE Transactions on Instrumentation and Measurement*, vol. 60, no. 11, pp. 3534–3546, 2011.
- [8] P. Hinterseer, S. Hirche, S. Chaudhuri, E. Steinbach, and M. Buss, "Perception-based data reduction and transmission of haptic data in telepresence and teleaction systems," *IEEE Transactions on Signal Processing*, vol. 56, no. 2, pp. 588–597, 2008.
- [9] O. Dabeer and S. Chaudhuri, "Analysis of an adaptive sampler based on weber's law," *IEEE Transactions on Signal Processing*, vol. 59, no. 4, pp. 1868–1878, 2011.
- [10] A. Bhardwaj, O. Dabeer, and S. Chaudhuri, "Can we improve over weber sampling of haptic signals?" in *Information Theory and Applications Workshop (ITA)*, 2013. IEEE, 2013, pp. 1–6.
- [11] X. Xu, B. Cizmeci, C. Schuwerk, and E. Steinbach, "Haptic data reduction for time-delayed teleoperation using the time domain passivity approach," in *IEEE World Haptics Conference (WHC)*, 2015, pp. 512–518.
- [12] T. Nakano, S. Uozumi, R. Johansson, and K. Ohnishi, "A quantization method for haptic data lossy compression," in *2015 IEEE International Conference on Mechatronics (ICM)*, 2015, pp. 126–131.
- [13] ns3, "The network simulator," 2011. [Online]. Available: <http://www.nsnam.org/>
- [14] D.-M. Chiu and R. Jain, "Analysis of the increase/decrease algorithms for congestion avoidance in computer networks," *Computer Networks and ISDN Systems*, vol. 17, no. 1, pp. 1–14, 1989.
- [15] S. Chaudhuri and S. Chaudhuri, "Volume preserving haptic pottery," in *IEEE Haptics Symposium (HAPTICS)*, 2014, pp. 129–134.